Computers in Industry 151 (2023) 103984

Contents lists available at ScienceDirect

Computers in Industry

journal homepage: www.sciencedirect.com/journal/computers-in-industry

Learning human-process interaction in manual manufacturing job shops through indoor positioning systems☆

Francesco Pilati *, Andrea Sbaragli

Department of Industrial Engineering - University of Trento, via Sommarive 9, 38123 Trento, Italy

ARTICLE INFO

Keywords:
Indoor positioning systems
Operator 4.0
Industrial DB scan
Manual manufacturing processes
Machine learning

ABSTRACT

Nowadays, manufacturing systems are increasingly embracing the Industry 4.0 paradigm. Therefore, manual and low-standardized manufacturing environments are often digitized through Industrial Internet of Things technologies to quantitatively assess and investigate the role of the human factor from multiple points of view. This approach is commonly known as Operator 4.0. In such a scenario, this manuscript proposes an original digital architecture to monitor the efficiency and the social sustainability of labor-intensive manufacturing job shops. While the anonymous spatio-temporal trajectories of tagged workers are acquired through an ultrawide band radio network, machine learning algorithms autonomously detect the human-process interactions with strategic industrial entities upon developing industrial key performing indicators. The proposed architecture is tested and validated in a real manual manufacturing system. In detail, the performing accuracies of the machine learning-based software provide industrial plant supervisors with several production metrics to identify the hidden weaknesses and bottlenecks of the monitored manufacturing system. Such digital assessment may trigger a re-organization of the considered process to, for instance, enhance the allocation of the material in storage areas while fairly re-balancing the distances traveled by workers for picking activities.

1. Introduction

The Industry 4.0 paradigm is progressively powering different technological advances in manufacturing systems to increase in-plant productivity by merging together digital and physical worlds. In such a widespread integration, any industrial entity is connected to the Internet enabling data gathering and if necessary triggering automatic process modification (Pereira and Romero, 2017). This approach is leading to smart and decentralized production environments. However, the full automation of processes is not always feasible or economically viable, especially for small and medium enterprises (SMEs) (Bortolini et al., 2021). Therefore, Industrial Internet of Things (IIoT) technologies enrich industrial digitization by acquiring large volumes of data from heterogeneous physical entities (Boston-Consulting-Group, 2022). These reliable datasets digitally back up an even more performing decision-making process by constantly updating manufacturing information systems (e.g., MES, ERP, etc.) (Yao et al., 2019). Considering low-standardized and variable environments, human workers are privacy-compliant digitized through different sets of IIoT wearables and sensors. This approach, known as Operator 4.0, mitigates processes' uncertainties and complements the workforce their pivotal role while performing extremely value-added activities in production cycles (Pilati et al., 2020). Different approaches have been proposed to smooth the mutual collaboration between industrial entities and workers (Romero et al., 2016). For instance, markerless motion capture (MOCAP) cameras and smart Radio Frequency Identification (RFID) glovers are leveraged to evaluate the postures of workers during assembly activities and perform an activity segmentation of task executions, respectively (Pilati et al., 2020; Singh et al., 2019). The relevance of such human-centered digital solutions is additionally remarked by the Industry 5.0 paradigm. Based on this, digital IIoT technologies are empowered by ML methods to mitigate different sets of challenges from supply chain disruptions to the aging of the European population (Directorate-General for Research and Innovation, 2021).

In such a digital scenario, indoor positioning systems (IPS) represent an active research field from health care to retail (Shum et al., 2022). Among the several communication protocols proposed so far, the ultrawide band (UWB) emerges as the best candidate in indoor and non-line-of-sights environments where different types of noise (e.g., jamming, scattering, etc.) and obstructions between receivers and

☆ This work has been supported by the project "SHIELD4US- Working safely COVID19" and cofounded by the Valorizzazione Ricerca Trentina (VRT) foundation with call entitled "Innovation for market launch 2020" of 4 December 2020.

* Corresponding author.
E-mail address: francesco.pilati@unitn.it (F. Pilati).

https://doi.org/10.1016/j.compind.2023.103984
Received 31 May 2023; Accepted 22 June 2023
Available online 5 July 2023

transmitters may occur (Santoro et al., 2022). The positioning capabilities of this technology are increasingly exploited in manual and low-standardized manufacturing systems to monitor the dynamic locations assumed by moving industrial entities during working shifts (Pilati et al., 2022). The areas of application range from process monitoring to safety management both for in-plant logistics and production. Therefore, industrial plant supervisors may enhance the visibility of labor-intensive processes by targeting different viewpoints from forklift overall equipment effectiveness and product throughput times to collision avoidance between automated guided vehicles (AGVs) and workers (Rácz-Szabó et al., 2020).

The digitization and thus the acquisition of vast datasets of production plants is contributing to achieving an increasingly performing data analytics process even for manufacturing systems. In detail, machine learning (ML) techniques represent an enabling factor to gain a competitive edge in modern and volatile industrial contexts. According to the Mckinsey Global Institute (Mckinsey&Company, 2022), in 2021 private companies invested 93.5 billion in such field doubling the 2020 level. While training processes of ML algorithms are constantly shortened, the 51% of European companies are involved in this rapid expansion and adoption. Benefitting from these advanced mathematical methods, surveyed adopters were able to save up to 90% of their operating cost whilst increasing up to 75% of their revenues. In modern and digitized manufacturing systems, supervised learning approaches may be leveraged to reduce inefficiencies and identify the best selection of manufacturing parameters to reduce process' wastes (Gönnheimer et al., 2022; Rajpathak et al., 2020). Similarly, unsupervised learning methods cluster spatio-temporal trajectories. Indeed, human activities are detected and thus assigned to known points of interest (Xiang et al., 2016).

Considering the analyzed scenario, this manuscript proposes an integrated hardware (HW) and software (SW) architecture to detect human-process interactions (HPIs) in manual and low-standardized job shops. From a manufacturing point of view, an HPI occurs whenever workers perform manual activities in machines or workbenches and pick or deposit materials in stock-keeping units (SKUs) of storage areas. While the HW part consists of an UWB-based IPS network where human workers are equipped with anonymous wearables tags, the ML-based SW exploits both supervised and unsupervised ML algorithms to achieve strategic key performing indicators (KPIs) of the manufacturing process (e.g. resource utilization ratio). These KPIs, displayed in an industrial dashboard, evaluate the efficiency and the social sustainability at the job shop, resource, and operator levels. Such IIoT and ML-based information enhance the industrial decision-making process by identifying hidden weaknesses and bottlenecks. In addition, the proposed digital architecture is very practical instead of tagging process entities with RFID technology. Based on this aim, the manuscript is organized as follows. Section 2 describes the adoption of UWB-based IPS networks along with supervised and unsupervised learning applications to detect HPIs with industrial entities and increase the consistency of the decision-making process for manual manufacturing systems, respectively. The novelty of this work is the digital architecture (Section 3). In this regard, data collected by an UWB-based IPS are leveraged by ML methods to detect HPIs over shifts. The proposed digital architecture is validated in an operating manufacturing job shop (Section 4). Section 5 presents the developed KPIs to monitor the manufacturing systems from different viewpoints and levels of detail. Finally, Section 6 ends this manuscript by outlining the conclusions and further research opportunities.

2. Literature review

Regardless of the adopted manufacturing system configuration such as cellular or reconfigurable, the human factor still delivers strategic added values to the productive cycle (Wan and Leirmo, 2023). In such modern environments, the workforce represents the most flexible resource due to its ability in performing heterogeneous manufacturing tasks. Indeed, while a specific machine configuration processes limited families of products, workers have intra-cell assignments which increase manufacturing interdependencies and variability (Albini et al., 2023; Bortolini et al., 2020). Based on this, different applications aimed at digitizing the human factor with IIoT technologies in modern manufacturing systems gained consistent interest (Zamora-Hernández et al., 2021). This trend, defined as Operator 4.0, may bring competitive advantages to modern manufacturing systems. First, industrial plant supervisors perform a quantitative decision-making process based on digital data to enhance the as-is scenario under different viewpoints. For instance, the physical workload of human workers may be lowered or fairly rebalanced while increasing production efficiencies Second, gamification approaches may be implemented to promote and support human commitment and exchange of concerns and knowledge. Third, augmented reality applications might shorten workforce training periods and improve workstations' design and layout to achieve socially sustainable industrial environments (Romero et al., 2018, 2017; Marino et al., 2021). A further emphasis on social sustainability in human-centered manufacturing environments is brought by Industry 5.0. This primary concern on human factors increases the long-term well-being of workers by reducing internal turnover. Consequently, labor-intensive manufacturing settings benefit from increased in-plant productivity as a primary positive externality (Directorate-General for Research and Innovation, 2021; European Commission and Directorate-General for Research and Innovation and Müller, 2020).

Among the key enabling technologies to achieve the Operator 4.0 concept, IPSs are increasingly adopted in modern manufacturing systems to monitor the dynamic indoor positions of moving physical entities (Ruppert et al., 2018). Over the past decades, different communication protocols have been proposed and validated to achieve this challenging aim. Radio-frequency (RF) based protocols are less prone to interference than ultrasonic, optical and infrared devices. Considering the RF applications, both narrowband and wideband are adopted to indoor locate manufacturing entities. In such a vast area, the UWB radio emerges as the most accurate candidate due to its technical characteristics. In detail, the multipath resolution and bandwidth prevent signals from overlapping jamming, respectively (Mazhar et al., 2017; Santoro et al., 2021). Despite the communication protocol selection, IPSs' HW is distinguished by two main physical entities. The tags send positioning information with a given frequency rate to a network of reference points, the anchors (ANs). The ANs, in addition to defining the coverage area to be monitored, calculate the time-dependent positions assumed by moving entities equipped with tags. The Time Difference of Arrival (TDoA) geometrical methods is the most adopted to achieve this purpose (Santoro et al., 2022).

In such a digital scenario, there are different contributions aimed at leveraging positioning data to enrich manufacturing systems functioning from different viewpoints. Potential applications are to indoor position industrial entities. For instance, tagging products represent a privileged opportunity to reveal weak spots in production by comparing the expected throughput times with the real ones. Indeed, industrial plant supervisors may trigger production system modifications such as line rebalancing to increase the performance of assembly operations (Slovák et al., 2019). Automated forklifts and AGVs are tagged as well to evaluate the efficiency in picking and depositing routes and prevent potential collision sources (Lee et al., 2017; Sun et al., 2019). Despite the tangible benefits of such approaches, their strong limitation is not achieving the Operator 4.0 concept. To target this purpose, privacy and labor union concerns have to be properly considered and addressed (Acquisti et al., 2015). Based on this, the vast majority of contributions that leverage indoor positions of the workforce is focused on the safety management research area. Representative applications are the collision avoidance between operators and AGVs, and COVID-19 transmission prevention (Löcklin et al., 2022; Pilati et al., 2022). To avoid these concerns and monitor low standardized process efficiency,

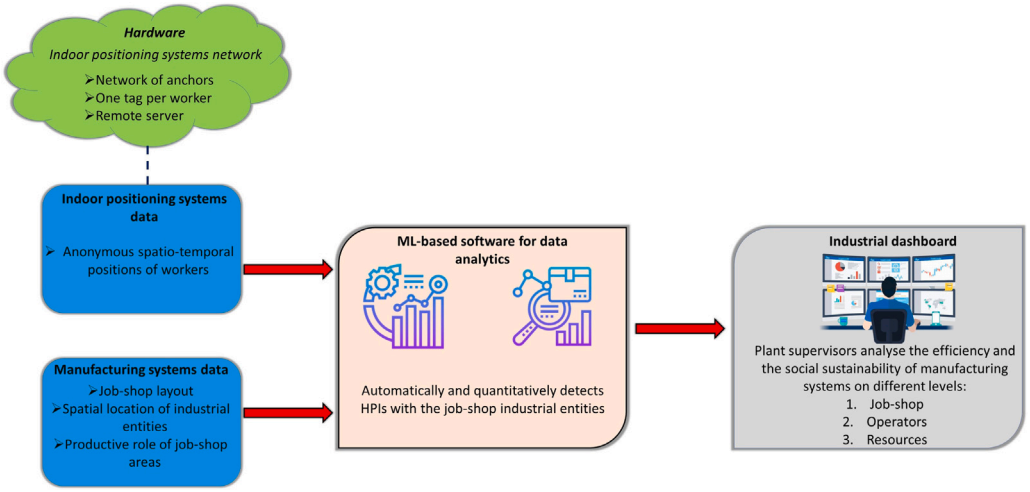

Fig. 1. Overview of the proposed digital architecture. (For interpretation of the references to color in this figure legend, the reader is referred to the web version of this article.)

several applications tag industrial entities utilized by workers during task executions. For instance, exploiting the indoor position of manufacturing shared tools enables to reduce searching times and assess their utilization ratio (Kelepouris and McFarlane, 2010). Similarly, manual forklifts' picking and depositing performances are evaluated as well Gladysz et al. (2017). However, the analyzed IPS-based contributions do not exploit clustering algorithms to mine value in acquired spatio-temporal data. In manufacturing environments, Darányi et al. (2022) adopt a fuzzy logic approach to improve tools management. Though, the presented approach does not outline the obtained accuracies to cluster tools' job shop positions in the spatial and temporal dimensions, potentially leading to not representative industrial KPIs such as utilization ratios. Therefore, to enhance data analytics processes, machine-learning methods are increasingly adopted to mine value in data acquired by IIoT technologies (Albanese et al., 2022). In this regard, several unsupervised spatial clustering techniques have been proposed. For instance, from data acquired by the Global Positioning System, spatial patterns in human trajectories are exploited to gain strategic insights about the performed activities in given time windows. Hence, times spent in a given geographical location of interest are automatically evaluated (e.g. supermarket, restaurant, etc.) (Xiang et al., 2016; Kanagala and Krishnaiah, 2016). However, these approaches are insensitive to the temporal dimension and thus utterly inadequate in industrial environments. Indeed, manufacturing interactions occurring in the same geometric regions but in different time windows may be merged together leading to skewed KPIs.

To overcome the mentioned limitations, this manuscript proposes a novel digital architecture to achieve an UWB-based Operator 4.0 concept in low-standardized and labor-intensive manufacturing systems. In addition, the data analytics process is enriched by the Industrial DB scan, an original unsupervised learning spatial clustering technique to detect HPIs with relevant industrial entities. Finally, the proposed approach automatically assesses multi-dimensional KPIs upon industrial plant supervisors can detect weaknesses and bottlenecks of the considered manufacturing job shop. In addition, the social sustainability of workers is analyzed by evaluating the distances traveled during picking/deposit activities.

3. Digital architecture

This section represents the original proposal of the manuscript. First, the General Data Privacy Regulation (GDPR)-compliant HW part of the developed architecture tags industrial workers through an UWB-based IPS to anonymously acquire workers' trajectories during the working shift. Second, its ML-based SW counterpart leverages spatio-temporal and manufacturing systems data to detect HPIs with strategic industrial entities in manual and low-standardized productive processes. The proposed SW adopts both supervised and unsupervised methods to achieve a performing data analytics process. Finally, an industrial dashboard is developed to analyze through strategic KPIs the efficiency and social sustainability of manual manufacturing systems on three different levels of detail. Fig. 1 presents the overview of the briefly outlined digital architecture. In detail, while the green-colored cloud lists the core devices of the IPS-based HW, the spatio-temporal and manufacturing data to be fed into the ML-based software (e.g., pink box) are presented in blue. The grey box describes the industrial dashboard by listing the three different levels of detail, namely job-shop, operators and resources. Finally, Appendix section sums up the indices and parameters to ease the reading process of this quantitative Section.

3.1. Hardware

The developed HW is an UWB-based IPS that acquires the dynamic indoor spatio-temporal positions of tagged entities with a given average sampling frequency. The IIoT architecture is based on Decawave commercial modules and is composed of two main systems (Qorvo, 2022a,b). First, a set of ANs define the reference region in which are monitored the dynamic positions assumed by wearable and anonymous tags over working shifts. In detail, the UWB-based network of ANs estimates the dynamic positions assumed by tagged human operators over the shift through the TDoA ranging technique. This geometric method calculates the indoor spatio-temporal position of tags by the intersection of two hyperbolas from at least three active ANs (Santoro et al., 2022). Any AN is based on Raspberry PI 3 connected to a DWM1001 UWB-based radio module. These reference points have to be displaced on the ceiling of the manufacturing environment to be monitored with a distance between each other at greatest equal to 20 m (Fig. 2). This network is connected and hence synchronized through a common Wi-Fi access point. The compact wearables are based on Decawave DWM1001 SoM which is configured to use UWB Channel 5 with bandwidth and frequency of 499.2 MHz and 6489.6 MHz, respectively. In addition, the DWM1001 SoM integrates, among the others, a low-power Nordic Semiconductors nRF52 microcontroller. Data sharing and acquisition are achieved by exploiting the MQTT protocol to enable data transfer to the remote server.

3.2. Machine learning-based software for data analytics

Based on the features of the adopted UWB-based IPS network, this Section extensively describes the steps to leverage the acquired spatio-temporal positioning data in manual and low-standardized manufacturing systems distinguished by value-added areas in which workers

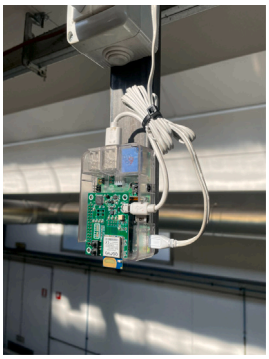

(a) Anchor mounted on the ceiling of an industrial building

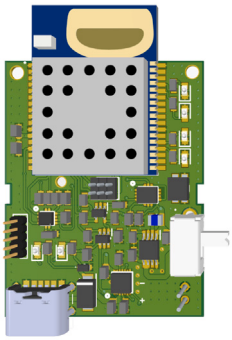

(b) Board of the tag worn by workers

Fig. 2. Adopted UWB-based IPS hardware.

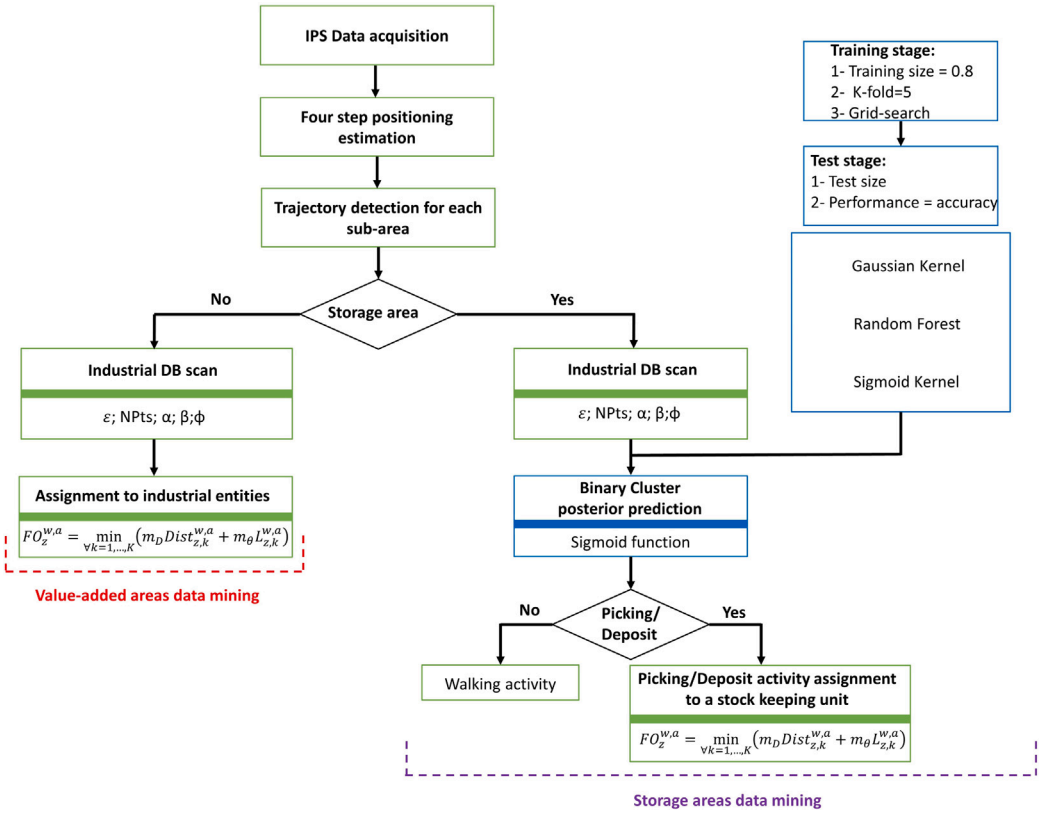

Fig. 3. Heuristic flow diagram of the developed ML-based software for data analytics.

perform manual operations and SKUs storage areas (Fig. 3). The goal of such analysis is to detect through the original Industrial DB scan manufacturing HPIs with industrial entities such as machines and SKUs to gain unprecedented visibility of manufacturing job shops. For instance, evaluating the utilization ratio of industrial entities and the distances traveled by workers during material replenishment. To ease the reading process, five sub-subsection outlines the key steps to be performed in order to meet such ambitious aims. In addition, Appendix lists the indices and parameters that will be introduced in the following lines.

3.2.1. Four step positioning estimation

Before starting the detection of HPIs, a pre-processing step has to be implemented to mitigate the intrinsic interference of manufacturing settings in the anonymous positioning data (Fig. 3). First, acquired data are processed by the Savitzky–Golay filter. This data smoothing method fits a discrete set of points into a polynomial curve of a chosen degree using an odd time window (Schafer, 2011). Second, the Cheng Filter (Cheng et al., 2020) detects and thus eliminates outliers whether the following condition is met (Eq. (1)).

$$|v_f^w - MAD^w| \geq v^{max} \tag{1}$$

Where v_f^w represents the velocity of the wth worker over the fth timeframe and MAD^w is the median absolute deviation with respect to velocities of the wth worker. Of course, v^{max} is a constant and has to be set appropriately based on the motion patterns of the monitored case study. This data removal is particularly relevant since the following unicycle Extended Kalman Filter is insensitive to outliers in human

trajectories (Antonucci et al., 2019). In particular, the forward prediction of the state during the fth timeframe given the previous one is computed as it follows(Eq. (2)).

$$x^{w}_{f|f-1} = \begin{bmatrix} px^{w}_{f-1} + \delta t v^{w}_{f-1} \cos\left(\theta^{w}_{f-1}\right) \\ py^{w}_{f-1} + \delta t v^{w}_{f-1} \sin\left(\theta^{w}_{f-1}\right) \\ \theta^{w}_{f} \\ v^{w}_{f} \end{bmatrix} + \begin{bmatrix} 0 & 0 \\ 0 & 0 \\ \delta t & 0 \\ 0 & \delta t \end{bmatrix} \begin{bmatrix} \eta\theta^{w}_{f-1} \\ \eta v^{w}_{f-1} \end{bmatrix} \quad (2)$$

Where θ^{w}_{f-1} and v^{w}_{f-1} represent the worker's trajectory angle and velocity during the time frame $f-1$. In addition, η represents the Gaussian distributed noise and δt describes the delta time between consecutive indoor positions. The last method of the pre-processing step is to perform a backward estimation of the state at the f-1 given the fth time frame through the Rauch–Tung–Striebel smoother (Miller, 2016).

3.2.2. Trajectory detection for each sub-area

After having performed the noise mitigation, the proposed original SW performs a trajectory detection for each operator and sub-area as depicted in Fig. 3. Over a defined monitoring period, the set $T = \{T^{w}, T^{w+1}, \dots, T^{W}\}$ groups sets of trajectories made by the W active workers. Considering whichever industrial job shop, its monitored area can be conceptually divided into A sub-areas based on their functional role in the manufacturing cycle. Where A represents the possible number of sub-areas that should be decided in agreement with industrial plant supervisors. Therefore, $T^{w} = \{t^{w,a}_{i}, t^{w,a'}_{i+1}, \dots, t^{w,a}_{I}\}$, where $t^{w,a}_{i}$ represents the ith sub-trajectory of the wth worker occurred in the ath area of the job shop. Based on this, $t^{w,a}_{1}$ and $t^{w,a'}_{2}$ are two consecutive sub-trajectories occurred in different sub-areas (e.g. $a \neq a'$). In addition, any $t^{w,a}_{i} = \{p^{w,a}_{i,f'}, p^{w,a}_{i,f'+1}, \dots, p^{w,a}_{i,f^*}\}$ is a structure where $p^{w,a}_{i,f} = (px^{w,a}_{i,f}, py^{w,a}_{i,f}, ts^{w,a}_{i,f})$ is a spatio-temporal point. In detail, any fth point belonging to a given $t^{w,a}_{i}$ must meet the following condition (Eq. (3)).

$$\forall\, 0 \leq f < f' \leq F \Rightarrow ts^{w,a}_{i,f'} > ts^{w,a}_{i,f} \quad (3)$$

Based on the computed $t^{w,a}_{i}$, the algorithm checks whether sub-trajectories belong to any storage area of the considered manual job shop. As outlined in Fig. 3, whenever this check is false, the SW automatically recognizes that the considered trajectory occurs in value-added areas and triggers two data mining steps, Industrial DB scan based, to detect HPIs with strategic industrial entities such as machinery and workbench (Section 3.2.3). Contrarily, supposing the sub-trajectory check is met, specific data mining steps are performed to detect HPIs in storage areas, namely picking/deposit activities in SKUs (Section 3.2.4).

3.2.3. Value-added areas data mining

Whenever human workers interact with the surrounding manufacturing resources, they perform strategic activities in front of it. Therefore, any HPI has the following characteristics: (1) its consecutive points have a high-spatial density and (2) the related duration is strictly greater than zero seconds. Based on these considerations, the following paragraph quantitatively describes the original Industrial DB scan developed to overcome the limitations outlined in Section 2. Let consider an arbitrary $t^{w,a}_{i}$ composed by a variable number of $p^{w,a}_{i,f}$. The ϵ temporal sequence of a given $p^{w,a}_{i,f}$ is the maximum number of points in $t^{w,a}_{i}$ that meet the following condition (Eq. (4)).

$$p^{w,a}_{i,f} \in \epsilon(p^{w,a}_{i,f}, d^*) \Leftrightarrow EuclideanDistance(p^{w,a}_{i,f}, p^{w,a}_{i,f'}) \leq d^*, \forall p^{w,a}_{i,f} \in t^{w,a}_{i} \quad (4)$$

where d^* describes the maximum radius to be considered. Supposing that in the ith sub-trajectory the former condition is verified for a variable number of points, let define the qth ϵ temporal sequence as $S^{w,a}_{i,q} = \{p^{w,a}_{i,f',q}, p^{w,a'}_{i,f'+1,q}, \dots, p^{w,a}_{i,f^*,q}\}$. However, the ϵ temporal sequence has to be consistent with the temporal dimension. The following Eq. (5) avoids considering two separate HPIs that occurred in the same region as one.

$$p^{w,a}_{i,f',q} - p^{w,a}_{i,f'+1,q} = \delta t, \forall\ p^{w,a}_{i,f',q}\ ,\ p^{w,a}_{i,f'+1,q} \in S^{w,a}_{i,q} \quad (5)$$

where δt represents the sampling time of the adopted HW. Finally, $S^{w,a}_{i,q}$ is a relevant HPI whether groups at least a total number of points equal to or greater than a threshold (NPts). This latter parameter is set based on human motion and may vary from sub-area to sub-area to increase the performance of the developed algorithm. However, the processed $p^{w,a}_{i,j,q}$ may be affected by the intrinsic uncertainty of human motion and other types of noise not properly mitigated during the pre-processing stage. Based on this, let consider two consecutive HPIs $C^{w,a}_{z,i}$ and $C^{w,a}_{z+1,i}$ for the first operator in the ath sub-area during the ith sub-trajectory. In detail, any $C^{w,a}_{z,i} = \{p^{w,a}_{i,f',z}, p^{w,a}_{i,f'+1,z}, \dots, p^{w,a}_{i,f^*,z}\}$. In addition, HPIs are also distinguished by a geometric center $O^{w,a}_{z,i} = \{Ox^{w,a}_{z,i}, Oy^{w,a}_{z,i}\}$ that can be calculated as the weighted average between the current acquired position ($px^{w,a}_{i,f',z}$) and the delta time between consecutive timestamps ($ts^{w,a}_{i,f'+1,z}$ and $ts^{w,a}_{i,f',z}$) (Eq. (6)).

$$Ox^{w,a}_{z,i} = \frac{\sum_{f=f'}^{f^*-1} px^{w,a}_{i,f',z}\left(ts^{w,a}_{i,f'+1,z} - ts^{w,a}_{i,f',z}\right)}{\sum_{f=f'}^{f^*-1}\left(ts^{w,a}_{i,f'+1,z} - ts^{w,a}_{i,f',z}\right)} \quad (6)$$

The same approach is adopted to calculate the y dimension of the center. In addition, from a temporal viewpoint $C^{w,a}_{z,i}$ and $C^{w,a}_{z+1,i}$ are spaced by a fixed duration in the preferred time unit. Therefore, two consecutive HPIs can be merged into a single one whether the Eq. (7) is met and at least one between Eq. (8) and (9) is true (Xiang et al., 2016).

$$ts^{w,a}_{i,f',z} - ts^{w,a}_{i,j^*,z+1} \leq \alpha \quad (7)$$

$$EuclideanDistance(p^{w,a}_{i,f',z}, O^{w,a}_{z+1,i}) \leq \beta \quad (8)$$

$$EuclideanDistance(p^{w,a}_{i,f',z}, p^{w,a}_{i,j^*,z+1}) \leq \phi \quad (9)$$

where α depends on the average time spent to travel from a process interaction to the following one and β and ϕ on the expected distance from consecutive stops. However, the detected HPIs provide no information on the manufacturing system because they are not related to any industrial entity and thus fail to develop industrial KPIs. In manufacturing environments, human operators perform certain activities of productive processes in known regions of job shops. These areas may be within the boundaries of machines, workbenches, etc. To this extent, let index as k these relevant industrial entities. Indeed, as depicted in Fig. 3, any detected $C^{w,a}_{z,i}$ can be assigned to one of them. To do so, a geometric entity representing any kth industrial resource and an objective function to be minimized have to be properly defined. Starting with the first, given the specific geometrical shape of the kth industrial entity, B_k represents its centroid. Then, the formulation of the objective function to assign any $C^{w,a}_{z,i}$ to a unique k follows. This assignment is based on distances and orientations. On one hand, the distance of the zth HPI from an arbitrary kth industrial resource is outlined in the Eq. (10).

$$Dist^{w,a}_{z,k} = \frac{\sum_{j=j''}^{j^*-1} dist(p^{w,a}_{i,f',z}, B_k)\left(ts^{w,a}_{i,f'+1,z} - ts^{w,a}_{i,f',z}\right)}{\sum_{j=j'}^{j^*-1}\left(ts^{w,a}_{i,f'+1,z} - ts^{w,a}_{i,f',z}\right)} \quad (10)$$

where $dist(p^{w,a}_{i,f'',z}, B_k)$ represents the Euclidean distance between the spatio-temporal point f' of the ith sub-trajectory of the zth HPI for the wth operator in the ath sub-area, and the centroid of the kth industrial resource. On the other hand, the orientation of each process interaction with respect to the kth industrial resource requires more computational steps. First, it is calculated $\theta^{w,a}_{i,f',f'+1,z}$ the angle assumed by the wth worker from the spatio-temporal point f' and $f'+1$. Second, $\theta^{w,a}_{i,f',k,z}$ represents the angle assumed by the same worker and the centroid of

the kth industrial entity. Therefore, Eq. (11) calculates the resulting orientation from the spatio-temporal point f' to the kth industrial entity.

$$L^{w,a}_{f',k} = |\theta^{w,a}_{i,f',k,z} - \theta^{w,a}_{i,f',f'+1,z}| \tag{11}$$

Finally, since HPIs group a variable number of spatio-temporal points, Eq. (12) evaluates the orientation of process interactions with respect to the kth industrial entity.

$$L^{w,a}_{z,k} = \frac{\sum_{j=f'}^{j^*-1} L^{w,a}_{i,f'} \left(ts^{w,a}_{i,f'+1,z} - ts^{w,a}_{i,f',z} \right)}{\sum_{j=f'}^{j^*-1} \left(ts^{w,a}_{i,f'+1,z} - ts^{w,a}_{i,f',z} \right)} \tag{12}$$

After having presented all the relevant parameters to perform the assignment of HPIs, the objective function to be minimized is outlined below (Eq. (13)).

$$FO^{w,a}_{z} = \min_{\forall k=1,\dots,K} \left(m_D Dist^{w,a}_{z,k} + m_\theta L^{w,a}_{z,k} \right) \tag{13}$$

where m_D and m_θ represent the weights connected to the distances and the orientations, respectively. Consequently, the remaining spatio-temporal points of a given sub-trajectory in value-added areas represent a walking activity for the considered human worker.

3.2.4. Storage areas data mining

Whether the detected sub-trajectory (see Section 3.2.2) occurs in storage areas, the original ML-based SW aims at detecting picking/deposit activities with SKUs (Fig. 3). Therefore, industrial plant supervisors can analyze in which SKUs anonymously tagged workers perform picking/deposit activities and thus evaluate the material allocation efficiency. To achieve this purpose, the first step to be performed is the Industrial DB scan. Despite the algorithm operatively works as outlined before, the hyper-parameters (e.g., ϵ NPts, α, β and ϕ) due to potentially different motion patterns may be indexed to a. Contrary to value-added areas, storage areas are generally wider in terms of square meters. Indeed, some HPIs detected by the developed Industrial DB scan may be false positives due to, among the others, the intrinsic uncertainty of human motion and noise of the signal acquired by the HW of the proposed digital architecture. For instance, the Industrial DB scan may label as process interactions trajectories instances in which the speed of worker motion decreased to overcome unexpected obstacles or aisles congestion. Based on this, a further processing step, supervised learning-based, is leveraged to avoid overestimations of HPIs leading to unrepresentative KPIs (Fig. 3). In detail, any $C^{w,a}_{z,i}$ is also distinguished by a mean velocity, acceleration, and duration (e.g., $\overline{v}^{w,a}_{z,i}$, $\overline{a}^{w,a}_{z,i}$ and $dur^{w,a}_{z,i}$). In addition, HPIs are manually assigned to class 1 whether, according to the collected ground truth, they cluster picking/deposit activities, 0 otherwise. Considering real manufacturing environments, collecting large video-based ground truth datasets may raise privacy and industrial secrets concerns of operators and companies, respectively. Another potential limitation is represented by the installation of cameras that may obstacle manual production routines. Therefore, a potential issue is represented by the limited dimension of ground truth datasets upon which training supervised ML models. In such a scenario, to maximize KPIs accuracies while limiting the intrusiveness of ground truth's video acquisitions, supervised-based ML algorithms can be easily trained with limited datasets compared to artificial neural networks (Albanese et al., 2021). Based on this, as depicted in Fig. 3, a Gaussian and Sigmoid Kernel, and a Random Forest are adequately trained using a shared approach. The 80% of the dataset represents the training set. In this heterogeneous set, a K-fold cross-validation and a grid-search approach are implemented. As a result, the proposed models are less biased and the hyperparameters optimized. While for the two kernels the hyperparameters to be optimized are γ and C, the Random Forest classifier has to optimize the number of estimators, the minimum sample splits and the number of features allowed. Then, the accuracies of the hyperparameters optimized classifiers are validated in the test set. After having learned the features connected to classes, the prediction stage can be triggered for whichever HPI returned by the Industrial DB scan in sub-trajectories of storage areas over working shifts. In detail, a Sigmoid function computes the posterior class probability for each classifier (Lin et al., 2007). Subsequently, these predictions are ensembled through a weighted average using classifiers accuracies as weights. Finally, the returned HPI is assigned to the class that has the highest probability. Whether the class is equal to 1, this picking or deposit activity has to be assigned to one of the SKUs belonging to the involved storage areas. According to Fig. 3, the assignment function follows the same approach outlined in Eq. (13). Otherwise, the HPI is considered a walking activity as the other instances of the sub-trajectories not previously labeled as HPIs by the Industrial DB scan.

3.3. Industrial dashboard

Benefitting from the aforepresented SW steps to mine value within UWB-based spatio-temporal trajectories, Table 1 summarizes how the time-dependent operations of monitored workers are classified during a standard working time window.

In detail, the SKU column has values greater than zero only if the related operation is a picking/deposit activity. Similarly, solely walking activities have distances traveled greater than zero meters. It is worth noting that this IIoT-based data may enrich the visibility of any manual and low-standardized job shop. Indeed, it is extremely useful to develop industrial KPIs upon with monitor the interdependencies, efficiency, and social sustainability of manufacturing job shops. The following bullet point list the strategic industrial metrics on three different levels of detail:

- **Job shop:** Operator activities timeline and segmentation; duration and number of picking/deposit activities in storage areas
- **Operators:** Distances traveled in picking/deposit activities; number of interaction with SKUs; from-to charts of traveling activities
- **Resources:** utilization ratio; usages overlapping

Based on the definition of these KPIs and levels of analysis, Fig. 4 outlines the developed industrial dashboard to achieve a user-friendly decision-making process. Plant supervisors have a unique opportunity to analyze processes' underperformance under different levels of detail. For instance, the job shop level of analysis may suggest that picking/deposit activities are not optimized due to poor material allocation. Despite this information being strategic to trigger a re-layout process, it fails to analyze an important negative externality. In this regard, the operators' level of detail evaluates the distances traveled by workers during picking/deposit activities to provide mainly two insights. First, a set of workers may be socially disadvantaged due to longer distances covered within the same shift. Second, these inconsistencies may be detected also comparing historical data of several different shifts.

To conclude this high-detailed and quantitative Section, the following lines combined with the nomenclature in Appendix highlight the key steps of the ML-based software for data analytics (Section 3.2). After the data acquisition of IPS-based historical data for a given working shift, the consistency of positioning data is improved with a four-step positioning estimation approach (Section 3.2.1). In this regard, the Savitzky–Golay and Cheng filters (Eq. (1)) perform data smoothing and outliers removal in operators' trajectories respectively. Then, the unicycle Extended Kalman filter (Eq. (2)) and Rauch–Tung–Striebel smoother further improve the acquired motion patterns. The resulting operators' trajectories are time-dependently indexed to a, the respective sub-areas of occurrence (Section 3.2.2). Based on a, each trajectory follows specific data mining steps as depicted in Fig. 3. On the one hand, whether the check on storage areas is not verified, two data mining steps are triggered to automatically detect HPIs with industrial resources (Section 3.2.3):

Table 1
Example of time-dependent working operation of a UWB tagged worker.

Start	End	Duration [sec]	Operation	SKU	Distance [m]
10:06:26.47	10:06:46.09	19.62	Workbench 1	0	0
10:06:46.76	10:06:51.36	4.60	Walking	0	3.4
10:06:51.59	10:06:53.83	2.15	Picking/Deposit	2	0
...	...	...	...	..	...
11:31:03.58	11:31:11.41	47.83	Machine 1	0	0

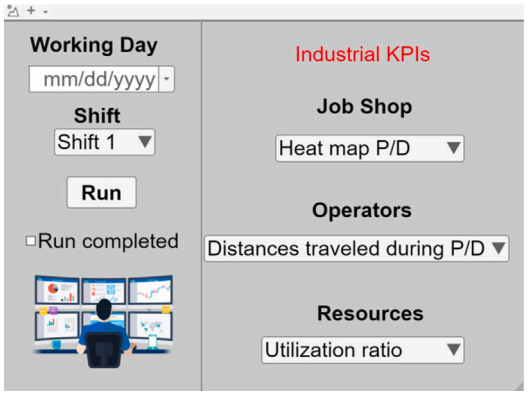

Fig. 4. Industrial dashboard.

- **Industrial DB scan**: based on the detailed formulation from Eq. (4) to Eq. (9), it triggers the detection of HPIs. However, such clustered positions provide little information on the system functioning since are not related to any industrial entity.
- **Assignment to industrial entities**: it defines an objective function to be minimized in order to assign HPIs to industrial entities based on distances and angles. From a geometric viewpoint, industrial entities are represented by a centroid.(e.g., from Eq. (10) to Eq. (13))

On the other hand, three data mining steps detect HPIs with storage areas' stock keeping units (Section 3.2.4):

- **Industrial DB scan**: this step follows the same mathematical formulation, exploiting identical input data. However, hyperparameters (e.g., ϵ NPts, α, β and ϕ) may be different due to potentially different operators' motion patterns in storage areas.
- **Binary Cluster posterior prediction**: benefitting from 3 trained ML-based classifiers (e.g., random forest, gaussian and sigmoid kernel), the detected HPIs are distinguished into walking or picking/deposit activities. To do so, the classifiers perform the posterior binary prediction through Sigmoid functions and ensembled using the weighted average (e.g., weights are the training accuracies). Finally, the HPIs are assigned to the activity that has the highest probability.
- **Picking/Deposit assignment to a stock keeping unit**: during this last step the P/D operations are assigned to SKUs following the same reasoning of before with industrial entities.

4. Case study & validation

The previously described digital architecture is tested and validated in a south-European manufacturing company that performs precision machining operations of components for the automotive industry. Fig. 5 depicts the layout of the monitored job shop in which two workers perform the manufacturing process. In such an environment, an agreement with industrial supervisors, the dedicated workforce, and the labor union is reached to achieve the Operator 4.0 concept. Indeed, workers wear on the preferred upper arm an anonymous UWB-based tag. Leveraging the developed digital architecture, plant supervisors require to evaluate the material allocation in storage areas at the detail level of each SKU and monitor the utilization ratio of industrial entities (e.g., workbenches and machines).

4.1. Architecture installation and job shop description

Before starting the experimental campaign, an extensive demonstratory period is focused on establishing trust among all shareholders. Based on this, laboratory tests are shown to workers to quantitatively back up the clear purpose of the analysis. Moreover, workers are fully compliant to sign the GDPR. In this non-binding agreement, they can revoke their consensus. Particular attention is focused on data storing and adequately blurring video-based ground truth. Finally, during the latest meetings, it is decided to leave six anonymous tags in the company's locker room to be autonomously equipped on the operators' preferred upper arm. Benefitting from this transparent process, all workers are fully compliant to be involved in the analysis. In addition, Fig. 5 shows the 2D geometrical positions of six ANs of the developed architecture having z-axis equal to 7.00 m. However, indoor positioning raw data with an average sampling rate equal to 20 Hz are highly affected by noise. In detail, the mean speed profile of workers is equal to 9.6 m/s. To increase the consistency of human motion patterns, the previously described four step positioning estimation methods (Section 3.2.1) are adopted resulting in a sampling rate and mean speed profile equal to 6.6 Hz and 1.3 m/s. Subsequently, based on the algorithm requirements, industrial supervisors decide to divide the monitored job shop into five sub-areas depending on their functional role in the manufacturing process (e.g., A = 5). The value-added area, namely the sub-area 1, hosts four different industrial entities and represents the most visited one by workers. In detail, workers load and unload into dedicated stand-alone machines (e.g., M1 and M2) different batches of materials and then perform manual manufacturing operations in the deburring and rectification workbenches (Fig. 6(b)). As depicted by Fig. 6(b), it is worth noting that the distances between the industrial entities combined with the high degree of freedom of human movements may considerably challenge the accuracy and reliability of the Industrial DB scan and the assignment of HPIs. In this area, industrial plant supervisors require to calculate the utilization ratio per worker of such entities and detect potential simultaneous usages of workbenches. Apart from the sub-area 5 which hosts two automatic lathes (AL) and the SKU ID 20 for scraps, the other three sub-areas stock different batches of materials. In particular, the fourth one groups SKUs of finished materials to be moved into other in-plant job shops by manual forklifts. The sub-area 2, partially depicted in Fig. 6(a) from a static viewpoint, stocks both finished and raw materials while the third one raw materials. Centroids of the SKUs are depicted through green dots in Fig. 5. Based on the production schedule at the beginning of each working shift, workers are required to move as close as possible to sub-area 2 all SKUs containing the batch to be manufactured and empty SKUs in which store processed materials. Therefore, according to the outlined SW architecture, plant supervisors can digitally analyze the efficiency of such material allocation by monitoring picking/deposit activities in SKUs along with distances traveled in such routes. However, before starting to discuss the industrial KPIs in Section 5, two intermediate considerations are addressed. First, for the sake of clarity, Section 4.2 describes the ML-based SW for data analytics functioning on sub-trajectories. Second, Section 4.3 validates the performances of the ML-based SW based on the collected ground truth. This investigation plays a pivotal role in order to avoid unrepresentative and misleading industrial KPIs.

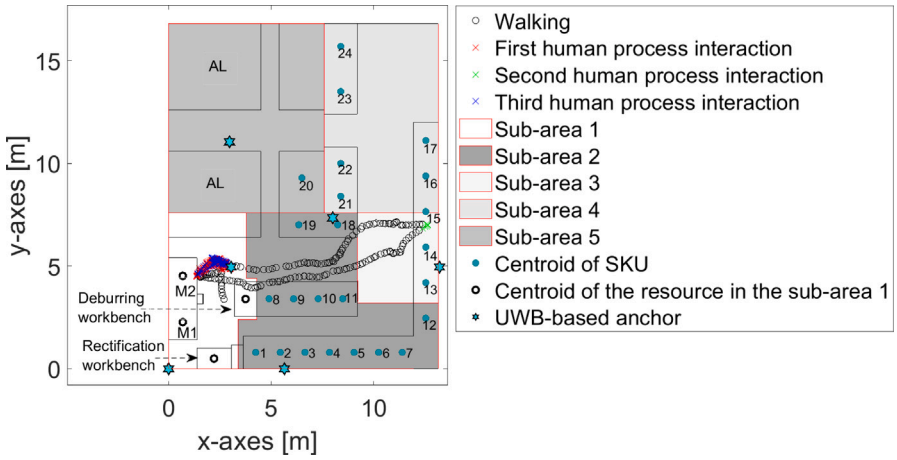

Fig. 5. Reference manual job shop of the manufacturing case study. (For interpretation of the references to color in this figure legend, the reader is referred to the web version of this article.)

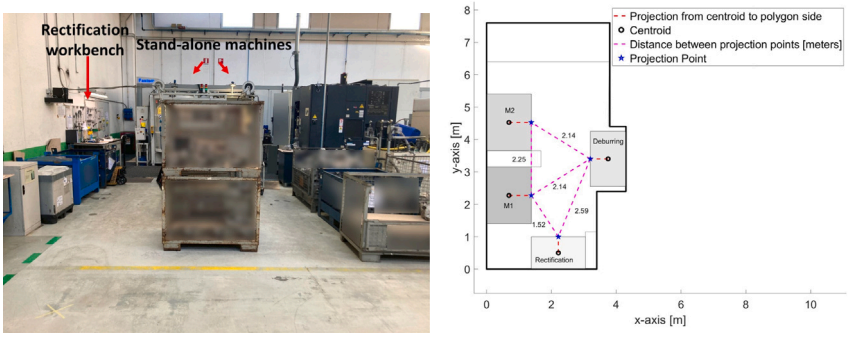

(a) Layout of the monitored manufacturing job-shop from a static point of view

(b) Geometry of the sub-area 1

Fig. 6. Manual industrial job shop.

4.2. Evaluation on sub-trajectories of ML-based software for data analytics

Benefitting from the algorithm functioning, Fig. 5 represents an example of HPIs detection in the manual and low-standardized job shop. The considered human movement occurred from 11:45:47 to 11:47:00 on the 15th of February 2021. According to the collected video-based ground truth, the operator 1 works in M2 for 38.71 s and then transiting through the sub-area 2 picks two raw materials from the SKU ID 15 and then goes back to M2 to load them in 15.74 s. As depicted in Fig. 5, the developed architecture detects three different process interactions. In the proposed example of five trajectories, the true positives and negatives are equal to 3 and 4, respectively. These instances represent a match between the actual scenario and the one determined by the developed algorithm. In this case of perfect detection, both false positives and negatives are equal to zero. For the sake of completeness, a false positive takes place whenever the Industrial DB scan clusters noise points into a not expected HPI. The false negatives represent the opposite condition. For simplicity, it is assumed that the three returned stops are the first three detected in the monitoring period. Indeed, $C_{1,1}^{1,1}$ and $C_{3,5}^{1,1}$ last 36.95 and 14.59 s, respectively. Therefore, the relative deviations of process interactions' duration are below 10%. In sub-area 3, a process interaction is detected, namely $C_{2,3}^{1,3}$. In particular, its input features (e.g., $\overline{v}_{2,3}^{1,3}$ and $\overline{a}_{2,3}^{1,3}$ and $dur_{2,3}^{1,3}$) are fed into the ensembled supervised learning classifiers to compute the posterior class probability. Since the resulting probability of class 1 is equal to the 80%, $C_{2,3}^{1,3}$ is classified as a picking/deposit activity. Despite no basis to better identify these two activities due to the intrinsic HW characteristics, the proposed digital architecture is much more practical and way less costly than tagging, using the RFID technology, products or industrial entities in modern manufacturing job shops. Finally, this process-driven activity is correctly assigned to the SKU ID 15. Despite the promising accuracies obtained by the ML-based SW in this set of spatio-temporal trajectories, the following subsection validates its performances with larger and representative ground truth datasets.

4.3. Performances of the ML-based software for data analytics

To adequately validate the performances of the ML-based SW, video-based ground truth is collected in 4 working shifts involving different workers. Considering the value-added area (e.g.,sub-area 1), 68 relevant stops occur with an aggregate length equal to 48.11 min. In addition, the data set is fairly balanced. While the percentages of HPIs that occurred in M1, M2, and deburring range from 25% to 30%, the rectification workbench hosts 20% of them. Based on the left part of Fig. 3, after the detection of T^w and the related sub-trajectories in sub-areas, the developed Industrial DB scan is adopted to detect relevant HPIs using NPts and ϵ equal to 15 and 0.17 m, respectively. In addition, α is equal to 1 s and β and ϕ to 0.5 m. These latter parameters are responsible for merging consecutive process interactions. The Industrial DB scan accuracies are evaluated through two metrics. First, a confusion matrix is developed to evaluate detection performances. The resulting accuracy over the 68 HPIs is equal to 82%. Second, the comparison between expected and returned process

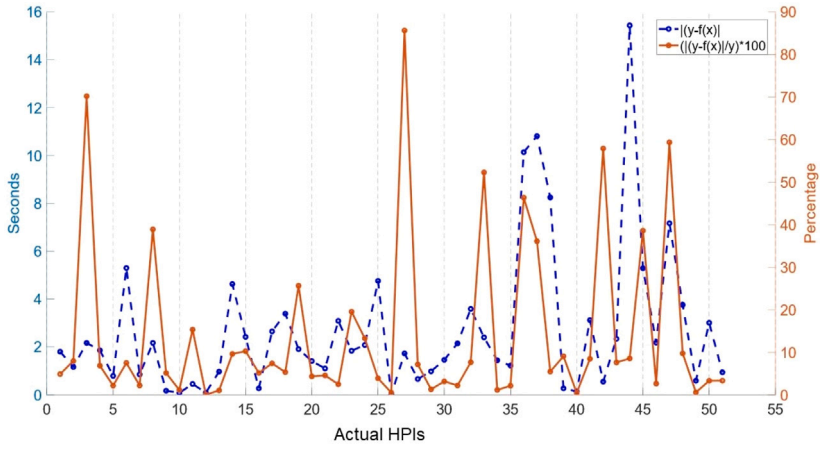

Fig. 7. Temporal performances of HPIs' detection of the developed architecture.

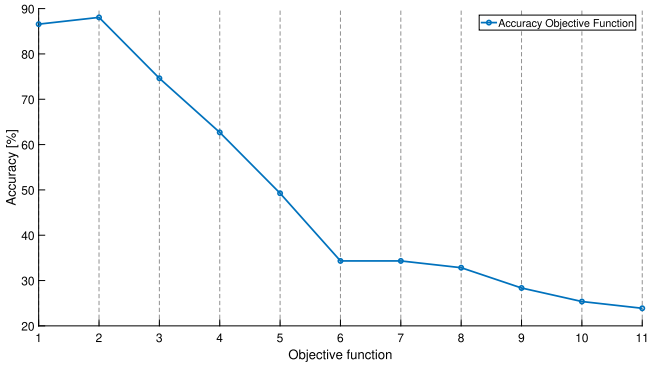

Fig. 8. Objective functions accuracies in HPIs' assignment.

interactions' duration is evaluated. Fig. 7 depicts this temporal analysis through the absolute and relative deviation of process interactions' duration. The data set considers solely the true positives that are equal to 51 relevant process interactions. In detail, the mean absolute and relative deviations are equal to 2.69 s and 14.14%, respectively.

After having assessed the promising accuracies of the proposed Industrial DB scan in such a small area, HPIs have to be assigned to one of the four industrial entities shown in Fig. 6. Weights of the objective function in Eq. (13) are arrays of 11 rows with element values that range from 0 to 100. Of course, the element-wise summation has to be equal to 100. Fig. 8 shows the accuracies of the 11 objective functions to assign HPIs to industrial entities. In detail, the first and last objective functions give no relevance to the angle and distance, respectively. The highest accuracy equal to 88.1% is achieved by the second one with m_D and m_θ equal to 90 and 10, respectively.

The same approach is adopted for the four storage areas to test and validated the right part of the SW in Fig. 3 aimed at detecting picking/deposit. In contrast to sub-area 1, it is reasonable to expect much shorter HPIs in stocking areas. Indeed, the Industrial DB scan is adopted using the same hyper-parameters apart from NPts which is equal to 5. Based on the collected video-based ground truth in the same 4 working shifts as before, 44 different trajectories of picking/deposit activities for a total duration of 8.35 min are analyzed to validate the algorithm under different human motion patterns. The proposed Industrial DB scan returned 100 different HPIs in which all the expected relevant activities were detected. However, a problem of over-estimation occurs. In detail, 35% of returned interactions are not related to the monitored manufacturing cycle. Among them, there are unexpected process interactions of human operators driven by different causes (e.g., unexpected obstacles). For this purpose, supervised-learning techniques are leveraged to learn the movement patterns of this scenario using as input features $\overline{v}_{z,i}^{w,a}$ and $\overline{a}_{z,i}^{w,a}$ and $dur_{z,i}^{w,a}$. During the training stage, the most performing hyper-parameters combinations are evaluated for all classifiers. In detail, the two kernels share the same optimal γ value equal to 0.01 but they have different C values. The Gaussian and Sigmoid values of C are equal to 10 and 1, respectively. On the other hand, the Random Forest is optimized under other sets of hyperparameters. The best configuration has 50 estimators, a minimum sample split of 0.6 and the features allowed are equal to the square root of the total number of features in the training data set. Then, the performances of the hyperparameters optimized classifiers are validated in the test set. While the Random forest has an accuracy of 71.4%, the accuracies of the Gaussian and Sigmoid Kernel are equal to 61.9% and 42.9%, respectively. The resulting accuracy of the weighted and Sigmoid-based ensembled classifier is equal to 76.4%. Finally, the objective function to be minimized performs the assignment of the detected HPIs to one of the SKU plotted in Fig. 6. Based on the available ground truth, this assignment solely depends on the distances with an accuracy of 100%.

5. Results & discussion

Based on the successful validation of the digital architecture (Section 4.3) in the mentioned manual and labor-intensive manufacturing job shop, this section presents the industrial KPIs to monitor the efficiency and the social sustainability with three levels of detail, as depicted by the industrial dashboard in Fig. 4.

5.1. Job shop level

The job shop dimension monitors from an aggregate viewpoint the functioning of the manual and UWB-referenced job shop. In particular, Fig. 9(a), depicts the monitored time window in which two anonymous operators equipped with their respective TagID are working within the coverage area defined by the displacement of ANs (Fig. 5), during the 3rd of March 2022.

In addition, Fig. 9(b) shows the time-dependent activities performed by workers from 11:03:00 to 11:09:00 on the monitored shift. While operator 2 mostly performs value-added operations in the deburring workbench, the other colleague performs several process-driven tasks. In particular, one picking/deposit activity and eight HPIs are automatically detected, where the vast majority of them occurs in M1. However, these first two KPIs fail to provide privileged insights for industrial supervisors' needs. Indeed, no evaluations regarding material allocations and resource utilization can be performed. Starting with the first aim, Fig. 10 shows through a dedicated color bar from white to red the aggregated picking/deposit interactions over the monitored

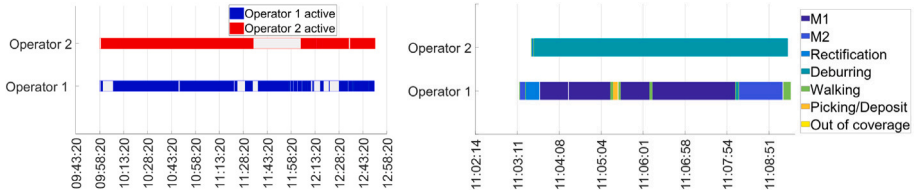

(a) Monitored time window of anonymous operators

(b) Time-dependent activities

Fig. 9. Temporal analysis of anonymous workers on the 3rd March 2022.

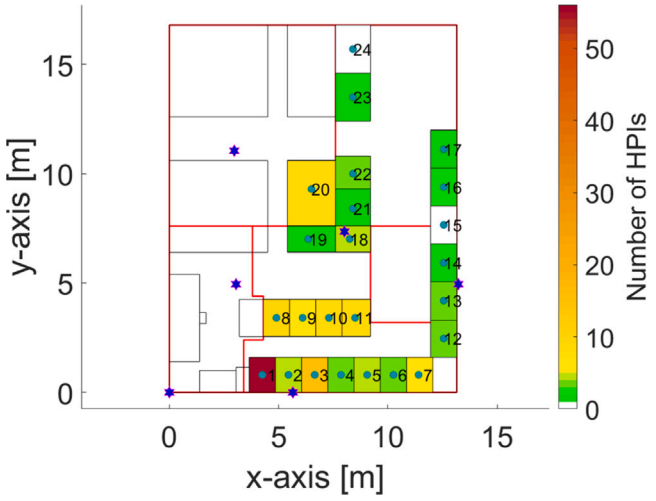

Fig. 10. Number of HPIs in storage areas during the monitored time window of anonymous workers on the 3rd March 2022. (For interpretation of the references to color in this figure legend, the reader is referred to the web version of this article.)

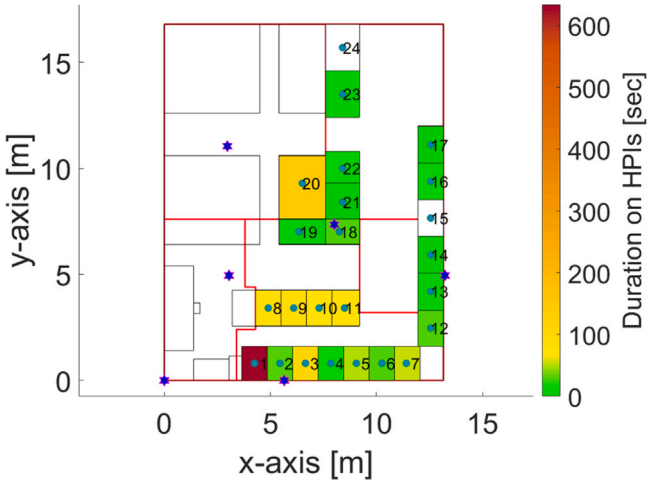

Fig. 11. Duration of HPIs in storage areas during the monitored time window of anonymous workers on the 3rd March 2022.

time window in SKUs. Benefitting from this, industrial plant supervisors can analyze the efficiency of the manufacturing systems during picking/deposit traveling activities. Fig. 10 suggests that the monitored manufacturing system is not optimized. Based on this, it is useful to consider the SKUs in the sub-area 2. The nearest SKUs to sub-area 1 host the highest picking/deposit activities. In detail, SKUs ID 1 and 3 have 56 and 15 visits over the monitored period, respectively. However, the farthest SKUs ID namely 5, 6, 7, 11, 12, and 18 register combined together 24 picking/deposit activities. This accounts for 18.6% of the total picking/deposit activities over the considered time period. Adopting the same approach with SKUs of other sub-areas, this metric increases to 26%. Therefore, almost a third of picking/deposit activities are inefficient.

In addition to this, Fig. 11 completes the analysis depicting the duration of HPIs activities in storage areas for both workers. During the monitored time period, the two anonymous workers spend roughly 25 minutes performing picking/deposit activities in storage areas. Based on the proposed heatmaps (Figs. 10 and 11), there is a clear direct correlation between the number of interactions with SKUs and the time spent performing picking/deposit activities. Indeed, as expected, SKU ID 1 shows the highest duration, accounting for 633.69 s. However, the underperforming material allocation in storage areas' SKUs can be analyzed on the temporal dimension as well. Considering the most inefficient SKUs of sub-area 2 (e.g., ID from 4 to 7, 11, 12 and 18), the total duration to perform/picking and deposit activities is equal to 250 seconds which accounts for the 16% of the total time to perform such process-driven activities. This statistic increases to the 30% by taking into account all SKUs belonging to other sub-areas.

This underperforming material allocation in storage areas triggers a consistent negative externality on meters traveled by workers. Indeed, to properly assess the impact on their manufacturing routines, the following subsection narrows the analysis to the Operators' level of detail.

5.2. Operators level

The picking/deposit activities of workers in defined SKUs show fairly similar percentages. While worker 1 visits 84 times the SKUs accounting for the 11% of his working routine, operator 2 performs 66 picking/deposit activities during the 7% of the monitored period. For both workers, several picking/deposit activities start and return in sub-area 1. Based on this, Fig. 12 outlines the meters traveled by workers to perform different activities in the manufacturing system (the acronyms A1 and P/D refer to the sub-area 1 and picking/deposit, respectively). While the total distances traveled over the monitored period by the two workers differ from 150 m, the comparison of travelings involving picking/deposit activities needs to be properly analyzed. Considering the traveling activities from sub-area 1 to a picking/deposit activity, operator 1, and operator 2 walk 207.47 and 193.28 m, respectively. Despite these metrics having similar values, the two workers perform highly different in-plant flows. Worker 1 and worker 2 travel from sub-area 1 to a given SKU 60 and 25 times, respectively. Indeed, worker 2 travels 2.24 times the meters of the other colleague, considering mean values.

Despite most of the time the two workers start the considered traveling route either from the rectification workbench or the deburring one, they show markedly different picking/deposit activities within the defined SKUs. To properly analyze and discuss this scenario, the 24 SKUs are divided into five classes. The "prime" class includes the SKUs 1,2,8. While the SKUs ID 3,4,9,10, and 19 belong to the "sub-optimal" class, the remaining SKUs of the sub-area 2 are grouped into

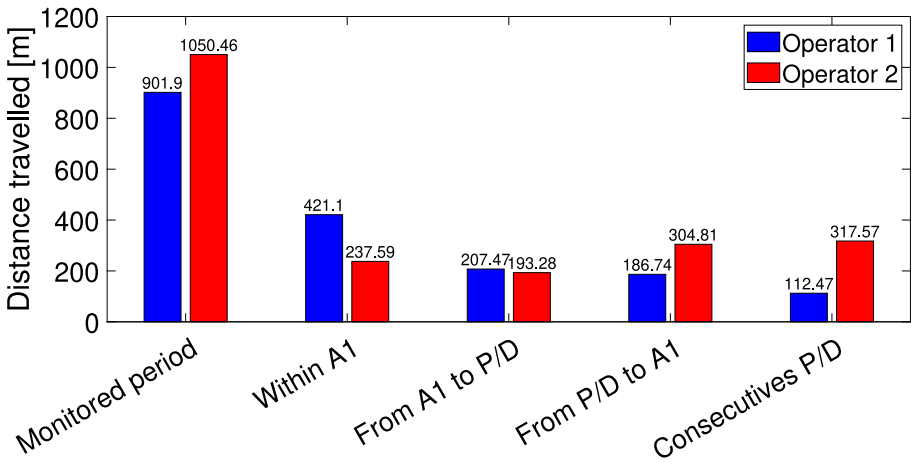

Fig. 12. Distances traveled by operators during the monitored period.

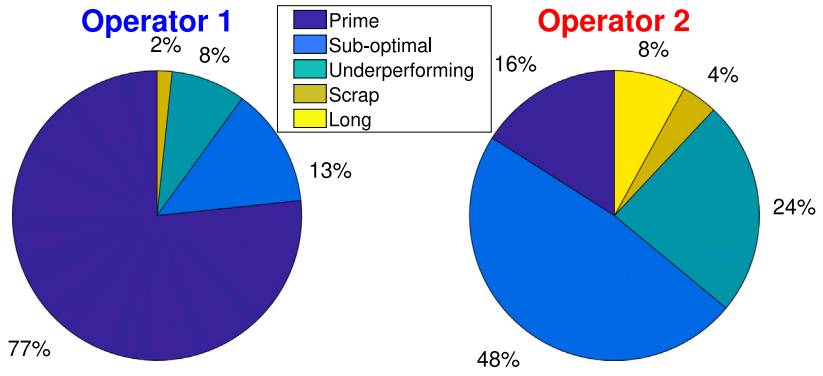

Fig. 13. Percentages for operators of picking/deposit activities from sub-area 1 divided by class of SKUs.

the "underperforming" one. Finally, all the other SKUs, apart from the 20 that belongs to the "scrap" class due to the intrinsic nature of material stored in it, are grouped in the class named "long". On one hand, worker 1 performs 43 picking/deposit activities in the "prime" class accounting for 72% of HPI in storage areas. In addition, 18% of flows happen in the "sub-optimal" SKUs. Among the other flows from the sub-area 1, solely 6 picking/deposit visits are towards the "long" class, accounting for 8% of the total activities in storage areas. The longest distance traveled is equal to 11.54 m and involves a flow from the rectification workbench to the SKU ID 20, most likely to deposit a manufacturing scrap. No flows from the sub-area 1 go to the "long" class. On the other hand, the picking/deposit activities of operator 2 from the sub-area 1 are completely different. Based on this, only 8% of flows are towards to SKU ID 1. In addition, while 14 flows go to the "sub-optimal" SKUs, 24% of total flows involve the "underperforming" class. The "long" class hosts 3 flows in the sub-area 5 to interact with the SKUs ID 22 and 23 (see Fig. 13).

According to these KPIs, worker 2 due to poor materials and thus SKUs allocation is socially disadvantaged. This scenario is completely similar when analyzing the number of flows with the distances traveled from picking/deposit activities to sub-area 1 and among consecutive picking/deposit activities. Regarding these latter flows, the evaluated KPIs suggest that operator 2 is also responsible for moving SKUs around the manufacturing job shop. While worker 1 performs the 80% of consecutive picking/deposit activities either in the "prime" class or with the "sub-optimal" one (e.g., from SKU ID1 to SKU ID 8, from SKU ID 1 to SKU ID 2, from SKU ID 3 to SKU ID 8, etc.), operator 2 travels between SKUs belonging to different sub-areas. Stark examples are represented by flows from SKU ID 7 to SKU ID 17 and to SKU ID 23. By comparing these sets of flows with the ones within the sub-area 1, it is clear how manual manufacturing systems rely on human commitment. Compared to SKUs that are dynamic entities, the four industrial entities have fixed locations defined by the aforementioned centroids (Fig. 6). Indeed, at mean values, worker 1 and worker 2 travel within the sub-area 1 1.57 and 1.64 m, respectively.

The acknowledgment of these inconsistencies in the monitored manual manufacturing system provides strategic insights to enhance the decision-making process. In particular, plant supervisors can re-balance the distances traveled by workers during picking/deposit activities. To achieve this aim, internal meetings may be organized to raise awareness among the workforce of efficient material allocation in storage areas. Focusing on the positive externality in reducing distances traveled, industrial plant supervisors may define specific guidelines to properly move as nearest as possible to the sub-area 2 the material batches to be manufactured during the shifts. According to the Operator 4.0 concept, a further incentive to meet this target is to design gamification approaches (Romero et al., 2016). For instance, workers that travel the shortest distances during picking/deposit activities may be awarded on a monthly basis. Therefore, the social sustainability of the considered low-standardized job shop is constantly reinforced at desired values while spreading the best practices among operators. Finally, based on supervisors' requests, the following subsection analyzes the resources' level of detail to point out their utilization ratio during the monitored time window.

5.3. Resources level

To properly assess the utilization ratio of resources, the focus is ensured on the workers' activities segmentation (Fig. 14). As depicted by the pie charts, operators 1 and 2 perform value-added activities for 56% and 62% of the entire time window interacting with the four industrial

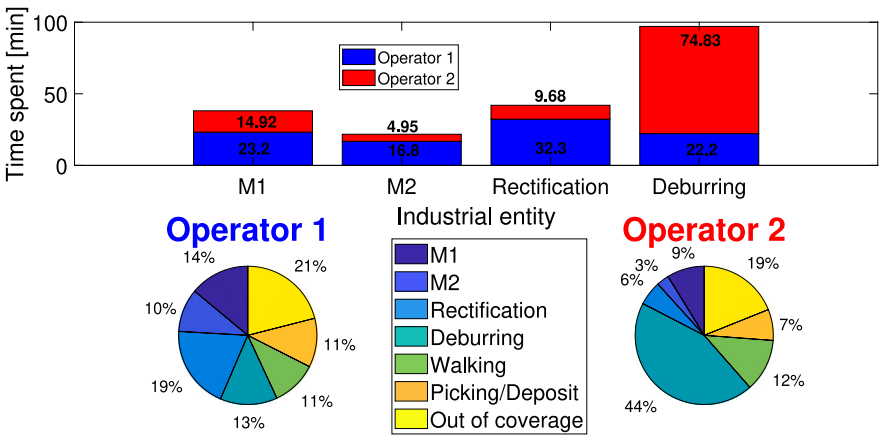

Fig. 14. Activities segmentation of the anonymous operator over the monitored time window.

entities (e.g., M1, M2, rectification, and deburring workbenches) in the sub-area 1, respectively. However, these two workers have different patterns of interaction with the entities. While the working percentages of worker 1 are fairly balanced among the four resources, the working times of operator 2 are distinguished by a markedly different pattern. Indeed, operator 2 for 74.8 min, that account for 44% of the entire working routine, performs materials deburring. These four resources are distinguished by a low utilization ratio. The deburring workbench registers the highest ratio equal to 55.9%. In addition, the monitored operators correctly parallelize their working routine by avoiding to occupy simultaneously the same resource. In this regard, a more performing material allocation may bring a further positive externality, namely a likely increase in the share of these value-added operations in the considered manufacturing process. Simultaneously, plant supervisors can combine the utilization ratio of industrial entities with manufactured goods to evaluate and compare the working efficiency of multiple working shifts.

For instance, a decrease in finished products can be analyzed through the different patterns of interactions with industrial entities. In such a scenario, it is reasonable to expect low utilization ratios of M1 and M2. At the same time, the deburring and the rectification workbenches may register high shares. Therefore, a likely root cause may be driven by poor automatic lathes' working quality potentially due to a worn tool.

To conclude, the proposed digital architecture can effectively support the labor-intensive and low-standardized job shops by creating value for its operational business. In particular, the adopted HW architecture combined with the ML-based SW enables a performing data analytics to enhance the visibility of the process functioning by minimizing installation costs compared to the RFID technology. Therefore, benefitting from the discussed multidimensional KPIs, industrial plant supervisors constantly analyze the in-plant operation and trigger target-oriented evaluations on processes' inefficiencies.

6. Conclusions & further research

Based on the Industry 4.0 paradigm, modern manufacturing systems are often addressing a digital decision-making process. In particular, labor-intensive environments digitize the human factor to achieve unprecedented insights into low-standardized production processes. In such a scenario, this manuscript proposes a digital architecture to assess the efficiency and the social sustainability of manual manufacturing job shops. In detail, an HW is developed as an UWB-based IPS in which a network of ANs defines the coverage area to be monitored over the working shift. The monitored operator wear on the preferred upper arm an anonymous TagID to acquire their spatio-temporal positioning during the production cycle execution. These geometric and privacy-compliant datasets are mined by an ML-based SW designed to monitor strategic KPIs of manual manufacturing job shops. For example, utilization ratios of industrial entities and distances traveled by workers during picking activities at the detail level of each SKU. The adopted ML algorithms are developed leveraging both supervised and unsupervised methods. On the one hand, an Industrial DB scan automatically detects HPIs to be assigned to the surrounding industrial entities (e.g., SKUs, stand-alone machines, etc.) through a tailored objective function to be minimized. On the other hand, three ensembled supervised classifiers remove the over-estimated picking/deposit activities driven by the intrinsic uncertainty of human motion in storage areas. This digital approach is tested and validated in a real and low-standardized manufacturing job shop that performs manual machining activities for the automotive industry in Southern Europe. During the labor-intensive productive cycle, the anonymous operators load and unload different batches of materials in stand-alone machines, and after automatic lathing operations perform manual deburring and rectifications. The experimental campaign shows promising accuracies of the proposed algorithms. In detail, considering sub-area 1, the Industrial DB scan correctly detects and assigns 82.0% and 88.1% of the expected HPIs to industrial entities considering the available ground truth, respectively. Regarding the interactions in storage areas, while the weighted ensembled classifier properly identifies 76.4% of the expected picking/deposit activities, the assignment to SKUs accuracy is equal to 100%. Benefiting from such promising accuracies, the developed digital dashboard shows strategic KPIs to assess the efficiency and the social sustainability of the considered manufacturing system. For instance, due to a weak material allocation in storage areas, worker 2 travels from sub-area 1 to the defined SKUs 2.2 times the meters of worker 1, resulting in a source of inefficiency and unfairness.

Further research opportunities should focus on different viewpoints. First, additional onboard sensors on the UWB tag such as IMUs may provide parameters to better classify the HPIs' motion patterns in storage areas. In this regard, reference systems (e.g. marked-based motion capture technologies) may be adopted to further evaluate the accuracy of the detected HPIs and related KPIs. Second, deep-learning networks may be leveraged to enhance the accuracy in classifying HPIs. In this regard, instead of representing interactions at aggregate levels, the classification is performed every time frame. Third, a decision support system may be developed to optimize humans' trajectory and thus embrace the cognitive feature of the Operator 4.0 concept. By doing so, targeted feedback would enhance the self-resilience of workers, an enabling characteristic of the Operator 5.0.

Declaration of competing interest

The authors declare that they have no known competing financial interests or personal relationships that could have appeared to influence the work reported in this paper.

Data availability

Data will be made available on request.

Acknowledgments

This work has been supported by the project "SHIELD4US- Working safely COVID19" and cofounded by the Valorizzazione Ricerca Trentina (VRT) foundation, Italy with call entitled "Innovation for market launch 2020" of 4 December 2020.

Appendix

This appendix provides the nomenclature, divided into indices and parameters, to ease the reading process.

Indices

$a, a' = 1, \dots, A$: sub-area of the monitored job-shop
$f, f', f^* = 1, \dots, F$: time frame
$i = 1, \dots, I$: sub-trajectory
$k = 1, \dots, K$: industrial entity
$w = 1, \dots, W$: tagged workers
$z = 1, \dots, Z$: stop

Parameters

α: greatest duration to merge consecutive stops
β: greatest distance between stops' centers to be merged
θ_f^w: angle assumed by the wth worker during the fth time frame
$\theta_{i,f',f'+1,z}^{w,a}$: the angle assumed by the wth worker from the point f' and $f'+1$ in the ath sub-area
$\theta_{i,f',k,z}^{w,a}$:represents the angle assumed by the same worker and the centroid of the kth industrial entity
η: Gaussian distributed acceleration noise
δt: sampling time of the adopted HW architecture
ϕ: greatest distance between the first and last point of stops to be merged
$\overline{a}_{z,i}^{w,a}$: : mean acceleration of the zth stop occurred in the ith sub-trajectory for the wth worker in the ath sub-area
B_k: geometric centroid of the kth industrial entity
$C_{z,i}^{w,a}$: zth stop occurred in the ith sub-trajectory of the wth operator in the ath sub-areas
d^*: greatest radius to create ϵ temporal sequences
$FO_{z,i}^{w,a}$: objective function to assign the zth stop occurred in the ith sub-trajectory for the wth worker in the ath sub-area to the kth industrial entity
$Dist_{z,k}^{w,a}$: Euclidean distance from the zth stop to the kth industrial entity for the wth worker in the ath sub-area
$dur_{z,i}^{w,a}$: duration of the zth stop occurred during the ith sub-trajectory for the wth worker in the ath sub-area
$L_{f',k}^{w,a}$: orientation during the fth time frame to the kth industrial entity for the wth operator in the ath sub-area
$L_{z,k}^{w,a}$: final orientation during the zth stop to the kth industrial entity for the wth operator in the ath sub-area
m_D: distance weight of the objective function
m_θ: orientation weight of the objective function
MAD^w: median absolute deviation of velocities of the wth worker
$NPts$: required number of points to create a stop
$O_{z,i}^{w,a} = \{Ox_{z,i}^{w,a}, Oy_{z,i}^{w,a}\}$: 2D center of the zth stop occurred in the ith sub-trajectory for the wth worker in the ath sub-area
$p_{i,f}^{w,a} = \{px_{i,f}^{w,a}, py_{i,f}^{w,a}, ts_{i,f}^{w,a}\}$: fth time frame of a spatio-temporal point belonging to the ith sub-trajectory of the wth worker in the ath area
$p_{i,f,q}^{w,a}$:fth time frame of a spatio-temporal point belonging to the ith sub-trajectory and qth ϵ temporal sequence of the wth worker in the ath area
$p_{i,f,z}^{w,a}$:fth time frame of a spatio-temporal point belonging to the ith sub-trajectory and zth stop of the wth worker in the ath area
$S_{i,q}^{w,a}$: qth ϵ temporal sequence occurred in the ith sub-trajectory for the wth worker in the ath sub-area
T: set of trajectories recorded
T^w: set of trajectories recorded for the wth worker
$ts_{i,f}^{w,a}$: timestamp of the ith trajectory during the fth time frame for the wth worker in the ath sub-area
$t_i^{w,a}$: ith sub-trajectory of the wth worker in the ath sub-area
v^{max}: greatest expected velocity of human walking
v_f^{max}: velocity of the wth worker during the fth time frame
$\overline{v}_{z,i}^{w,a}$: mean velocity of the zth stop occurred in the ith sub-trajectory for the wth worker in the ath sub-area
$x_{f|f-1}^w$: state of the model during the fth time frame given the f-1 for the wth worker

References

Acquisti, A., Brandimarte, L., Loewenstein, G., 2015. Privacy and human behavior in the age of information. Science 347 (6221), 509–514.
Albanese, A., Nardello, M., Brunelli, D., 2021. Automated pest detection with DNN on the edge for precision agriculture. IEEE J. Emerg. Sel. Top. Circuits Syst. 11 (3), 458–467.
Albanese, A., Nardello, M., Fiacco, G., Brunelli, D., 2022. Tiny machine learning for high accuracy product quality inspection. IEEE Sens. J. 1–9.
Albini, T., Brocchi, A., Murgia, G., Pranzo, M., 2023. Real-time optimization for a digital twin of a robotic cell with human operators. Comput. Ind. 146, 103858.
Antonucci, A., Magnago, V., Palopoli, L., Fontanelli, D., 2019. Performance assessment of a people tracker for social robots. In: 2019 IEEE International Instrumentation and Measurement Technology Conference. I2MTC, IEEE, pp. 1–6.
Bortolini, M., Botti, L., Galizia, F., Mora, C., 2020. Safety, ergonomics and human factors in reconfigurable manufacturing systems. In: Reconfigurable Manufacturing Systems: From Design to Implementation. Springer, pp. 123–138.
Bortolini, M., Faccio, M., Galizia, F.G., Gamberi, M., Pilati, F., 2021. Adaptive automation assembly systems in the industry 4.0 era: a reference framework and full–scale prototype. Appl. Sci. 11 (3), 1256.
Boston-Consulting-Group, 2022. Industry 4.0: The Future of Productivity and Growth in Manufacturing Industries. Tech. Rep. (Accessed 29 September 2022).
Cheng, L., Chang, H., Wang, K., Wu, Z., 2020. Real time indoor positioning system for smart grid based on uwb and artificial intelligence techniques. In: 2020 IEEE Conference on Technologies for Sustainability. SusTech, IEEE, pp. 1–7.
Darányi, A., Dörgő, G., Ruppert, T., Abonyi, J., 2022. Processing indoor positioning data by goal-oriented supervised fuzzy clustering for tool management. J. Manuf. Syst. 63, 15–22.
Directorate-General for Research and Innovation, 2021. Industry 5.0: towards a sustainable, human-centric, and resilient european industry. Tech. Rep., European Commission (Accessed 29 April 2023).
European Commission and Directorate-General for Research and Innovation, Müller, J., 2020. Enabling Technologies for Industry 5.0 : Results of a Workshop with Europe's Technology Leaders. Publications Office.
Gladysz, B., Santarek, K., Lysiak, C., 2017. Dynamic spaghetti diagrams. A case study of pilot RTLS implementation. In: International Conference on Intelligent Systems in Production Engineering and Maintenance. Springer, pp. 238–248.
Gönnheimer, P., Ströbel, R., Netzer, M., Fleischer, J., 2022. Generation of identifiable CNC reference runs with high information content for machine learning and analytic approaches to parameter identification. Procedia CIRP 107, 734–739.
Kanagala, H.K., Krishnaiah, V.J.R., 2016. A comparative study of K-Means, DBSCAN and OPTICS. In: 2016 International Conference on Computer Communication and Informatics. ICCCI, IEEE, pp. 1–6.
Kelepouris, T., McFarlane, D., 2010. Determining the value of asset location information systems in a manufacturing environment. Int. J. Prod. Econ. 126 (2), 324–334.
Lee, Y., Kim, J., Lee, H., Moon, K., 2017. IoT-based data transmitting system using a UWB and RFID system in smart warehouse. In: 2017 Ninth International Conference on Ubiquitous and Future Networks. ICUFN, pp. 545–547.
Lin, H.-T., Lin, C.-J., Weng, R.C., 2007. A note on Platt's probabilistic outputs for support vector machines. Mach. Learn. 68 (3), 267–276.
Löcklin, A., Dettinger, F., Artelt, M., Jazdi, N., Weyrich, M., 2022. Trajectory prediction of workers to improve AGV and AMR operation based on the manufacturing schedule. Procedia CIRP 107, 283–288, Leading manufacturing systems transformation – Proceedings of the 55th CIRP Conference on Manufacturing Systems 2022.
Marino, E., Barbieri, L., Colacino, B., Fleri, A.K., Bruno, F., 2021. An augmented reality inspection tool to support workers in Industry 4.0 environments. Comput. Ind. 127, 103412.
Mazhar, F., Khan, M.G., Sällberg, B., 2017. Precise indoor positioning using UWB: A review of methods, algorithms and implementations. Wirel. Pers. Commun. 97 (3), 4467–4491.
Mckinsey&Company, 2022. McKinsey Technology Trends Outlook 2022. Tech. Rep. (Accessed 29 September 2022).

Miller, J., 2016. Advanced stochastic modeling — jwmi.github.io. https://jwmi.github.io/ASM/index.html. (Accessed 31 August 2022).
Pereira, A.C., Romero, F., 2017. A review of the meanings and the implications of the Industry 4.0 concept. Procedia Manuf. 13, 1206–1214.
Pilati, F., Faccio, M., Gamberi, M., Regattieri, A., 2020. Learning manual assembly through real-time motion capture for operator training with augmented reality. Procedia Manuf. 45, 189–195.
Pilati, F., Sbaragli, A., Nardello, M., Santoro, L., Fontanelli, D., Brunelli, D., 2022. Indoor positioning systems to prevent the COVID19 transmission in manufacturing environments. Procedia CIRP 107, 1588–1593.
Qorvo, 2022a. Decawave DWM1000. https://www.decawave.com/product/dwm1000-module/. (Accessed 05 September 2022).
Qorvo, 2022b. Decawave DWM1001. https://www.decawave.com/product/dwm1001-module/. (Accessed 05 September 2022).
Rácz-Szabó, A., Ruppert, T., Bántay, L., Löcklin, A., Jakab, L., Abonyi, J., 2020. Real-time locating system in production management. Sensors 20 (23), 6766.
Rajpathak, D., Xu, Y., Gibbs, I., 2020. An integrated framework for automatic ontology learning from unstructured repair text data for effective fault detection and isolation in automotive domain. Comput. Ind. 123, 103338.
Romero, D., Bernus, P., Noran, O., Stahre, J., Fast-Berglund, Å., 2016. The operator 4.0: Human cyber-physical systems & adaptive automation towards human-automation symbiosis work systems. In: IFIP International Conference on Advances in Production Management Systems. Springer, pp. 677–686.
Romero, D., Mattsson, S., Fast-Berglund, Å., Wuest, T., Gorecky, D., Stahre, J., 2018. Digitalizing occupational health, safety and productivity for the operator 4.0. In: IFIP International Conference on Advances in Production Management Systems. Springer, pp. 473–481.
Romero, D., Wuest, T., Stahre, J., Gorecky, D., 2017. Social factory architecture: social networking services and production scenarios through the social internet of things, services and people for the social operator 4.0. In: IFIP International Conference on Advances in Production Management Systems. Springer, pp. 265–273.
Ruppert, T., Jaskó, S., Holczinger, T., Abonyi, J., 2018. Enabling technologies for operator 4.0: A survey. Appl. Sci. 8 (9), 1650.
Santoro, L., Nardello, M., Brunelli, D., Fontanelli, D., 2021. Scale up to infinity: The UWB indoor global positioning system. In: 2021 IEEE International Symposium on Robotic and Sensors Environments. ROSE, IEEE, pp. 1–8.
Santoro, L., Nardello, M., Fontanelli, D., Brunelli, D., Petri, D., 2022. Scalable centimetric tracking system for team sports. In: 2022 IEEE International Workshop on Sport, Technology and Research. STAR, IEEE, pp. 1–6.
Schafer, R.W., 2011. What is a Savitzky-Golay filter?[lecture notes]. IEEE Signal Process. Mag. 28 (4), 111–117.
Shum, L.C., Faieghi, R., Borsook, T., Faruk, T., Kassam, S., Nabavi, H., Spasojevic, S., Tung, J., Khan, S.S., Iaboni, A., 2022. Indoor location data for tracking human behaviours: A scoping review. Sensors 22 (3), 1220.
Singh, R.K., Michel, A., Nepa, P., Salvatore, A., 2019. Design of a compact yagi-uda antenna for near field UHF RFID smart gloves. In: 2019 IEEE International Conference on RFID Technology and Applications. RFID-TA, IEEE, pp. 453–457.
Slovák, J., Vašek, P., Šimovec, M., Melicher, M., Šišmišová, D., 2019. RTLS tracking of material flow in order to reveal weak spots in production process. In: 2019 22nd International Conference on Process Control. PC19, IEEE, pp. 234–238.
Sun, S., Hu, J., Li, J., Liu, R., Shu, M., Yang, Y., 2019. An INS-UWB based collision avoidance system for AGV. Algorithms 12 (2), 40.
Wan, P.K., Leirmo, T.r.L., 2023. Human-centric zero-defect manufacturing: State-of-the-art review, perspectives, and challenges. Comput. Ind. 144, 103792.
Xiang, L., Gao, M., Wu, T., 2016. Extracting stops from noisy trajectories: A sequence oriented clustering approach. ISPRS Int. J. Geo-Inf. 5 (3), 29.
Yao, X., Zhou, J., Lin, Y., Li, Y., Yu, H., Liu, Y., 2019. Smart manufacturing based on cyber-physical systems and beyond. J. Intell. Manuf. 30 (8), 2805–2817.
Zamora-Hernández, M.-A., Castro-Vargas, J.A., Azorin-Lopez, J., Garcia-Rodriguez, J., 2021. Deep learning-based visual control assistant for assembly in industry 4.0. Comput. Ind. 131, 103485.